CrossMark

ORIGINAL ARTICLE

High-uptake areas on positron emission tomography with the hypoxic radiotracer ^{18}F-FRP170 in glioblastomas include regions retaining proliferative activity under hypoxia

Takaaki Beppu · Toshiaki Sasaki · Kazunori Terasaki · Hiroaki Saura · Hideki Mtsuura · Kuniaki Ogasawara · Makoto Sasaki · Shigeru Ehara · Ren Iwata · Yoshihiro Takai

Abstract

Objective The aim was to evaluate the proliferative activity of high-uptake areas on positron emission tomography (PET) with the hypoxic cell radiotracer, 1-(2-[^{18}F]fluoro-1-[hydroxymethyl]ethoxy)methyl-2-nitroimidazole (FRP170).
Methods Thirteen patients with glioblastoma underwent FRP170 PET before tumor resection. During surgery, tumor specimens were stereotaxically obtained from regions corresponding to high (high-uptake areas, HUAs) and relatively low (low-uptake areas, LUAs) accumulation of FRP170. We compared immunohistochemical staining for Ki-67 and hypoxia-inducible factor (HIF)-1α between HUA and LUA.

Results HIF-1α index was significantly higher in HUAs than in LUAs. In contrast, mean Ki-67 indices did not differ significantly between HUAs and LUAs.
Conclusions Findings for HIF-1α index clearly indicated that HUAs on FRP170 PET represented hypoxic regions in glioblastoma. However, findings of Ki-67 index suggest that HUAs on FRP170 PET include regions retaining proliferative activity regardless of tissue hypoxia.

Keywords Glioblastoma · FRP170 · PET · Hypoxia · Proliferation

Abbreviation

FRP170	1-(2-[^{18}F]fluoro-1-[hydroxymethyl]ethyl)methyl-2-nitroimidazole
FDG	[^{18}F]fluorodeoxyglucose
FMISO	[^{18}F]fluoromisonidazole
Gd-T1WI	Gadolinium-enhanced T1-weighted imaging
HIF	Hypoxia-inducible factor
HUA	High-uptake area
LUA	Low-uptake area
MRI	Magnetic resonance imaging
ROI	Region of interest
PET	Positron emission tomography
VEGF	Vascular endothelial growth factor

T. Beppu (✉) · H. Saura · H. Mtsuura · K. Ogasawara
Department of Neurosurgery, Iwate Medical University,
Uchimaru 19-1, Morioka 020-8505, Japan
e-mail: tbeppu@iwate-med.ac.jp

T. Sasaki · K. Terasaki
Cyclotron Research Center, Iwate Medical University,
Morioka, Japan

M. Sasaki
Institute for Biomedical Sciences, Iwate Medical University,
Morioka, Japan

S. Ehara
Department of Radiology, Iwate Medical University,
Morioka, Japan

R. Iwata
Cyclotron and Radioisotope Center (CYRIC), Tohoku
University, Sendai, Japan

Y. Takai
Department of Radiology and Radiation Oncology, Hirosaki
University Graduate School of Medicine, Hirosaki, Japan

Introduction

Assessing hypoxic conditions in glioblastoma, as the most malignant type of brain tumor, is an essential means of determining the biological characteristics of the tumor. For example, hypoxia in glioblastoma activates hypoxia-responsive elements such as hypoxia-inducible factors

(HIFs), which lead to transcription of target genes including vascular endothelial growth factor (VEGF). VEGF induces angiogenesis and is also closely related to the proliferation and invasiveness of the tumor. Intratumoral hypoxic conditions are disadvantageous because relatively insufficient oxygen levels lead to low production of the peroxide radicals that induce DNA damage during radiotherapy [1, 2].

Positron emission tomography (PET) using hypoxic cell tracers offers an attractive method for detecting hypoxic cells because the modality is simple, minimally invasive, repeatable, and application is not limited to superficial tumors [3]. Hypoxic cells in brain tumors have already been detected using PET with some hypoxic cell tracers. We have previously reported on the assessment of hypoxic regions in glioblastoma using PET with 1-(2-[18F]fluoro-1-[hydroxymethyl]ethoxy)methyl-2-nitroimidazole (FRP170) [4–8]. Similar to [18F]fluoromisonidazole (FMISO) [9–11], FRP170 is synthesized from 2-nitroimidazole. Clarification of whether proliferative activity is retained in regions showing high accumulation of 2-nitroimidazole derivatives including FMISO and FRP170 on PET would provide useful information for various areas of clinical interest, such as targeting regions for biopsy or removal of tumor, and assessing the biological effects of radiation [12] and anti-VEGF antibody (bevacizumab) [13] which are closely associated with intratumoral hypoxia and proliferation. The current study assessed proliferative activity within tumor tissues showing high accumulations of FRP170 using immunohistochemical staining for HIF-1α as a marker of cell hypoxia and Ki-67 as a marker of cell proliferation. Some reports have investigated the relationships between hypoxia and proliferation or glucose metabolism in tumor tissues [10, 14–19], but this is the first report to compare areas of uptake on FRP170 PET with histological findings in patients with glioblastoma.

Materials and methods

Patients

The present study was performed in accordance with the precepts established by the Helsinki Declaration. All study protocols were approved by the ethics committee at our institute (No. H22-70). Patients recruited to this study were admitted to our institute between April 2008 and May 2014. Patients met the following entry criteria for the study: ≥20 years old with untreated glioblastoma localized to cerebral white matter other than the brainstem or cerebellum; data available from FRP170 PET; and tumor tissues obtained surgically according to the study protocol; and voluntary provision of written informed consent to participate. Preoperative diagnosis was based on the present history and findings from conventional magnetic resonance imaging (MRI) on admission, and the final diagnosis of glioblastoma was made based on histological features after surgery. Thirteen patients (9 men, 4 women; mean age, 60.3 ± 13.1 years; range 31–76 years) were enrolled after excluding patients who did not meet the entry criteria. The main location of the tumor was the frontal lobe in eight patients, temporal lobe in two patients, parietal lobe in two patients, and occipital lobe in one patient.

FRP170 PET

Within 7 days before surgery for tumor resection, conventional MRI including gadolinium-enhanced T1-weighted imaging (Gd-T1WI) and FRP170 PET were performed on different days. FRP170 was synthesized using on-column alkaline hydrolysis according to the methods described by Ishikawa et al. [5]. The final formulation for injection included normal saline containing 2.5 % v/v ethanol using solid-phase extraction techniques. Sixty minutes after intravenous injection of approximately 370 MBq (mean, 5.9 ± 1.8 MBq/kg) of FRP170, PET was performed using a PET/computed tomography system (Eminence Sophia SET3000 GCT/M; Shimadzu, Kyoto, Japan). PET scans were reconstructed using Fourier rebinning (FORE) + ordered subset expectation maximization (OSEM) with 4 iterations and 26 subsets, with the following conditions: field of view 256 mm^2, matrix 128 × 128, pixel size 2.0 × 2.0 mm^2, and slice sickness 2.6 mm. On FRP170 PET, regions of interest (ROIs) 10 mm in diameter were placed on areas of high accumulation (high-uptake areas, HUAs) and relatively low accumulation (low-uptake areas, LUAs) within the tumor and apparently normal cerebral white matter in the contralateral hemisphere, using the methods applied in our previous study [4]. Before obtaining ROIs, we determined the cutoff SUV for differentiation of HUAs from other areas using the following method. We manually changed the cutoff value to between 1.3 and 5.0 to determine the appropriate value in each patient, while observing changes in the width of the red-colored HUA on FRP170 PET. When the red-colored HUA was around 10 mm in diameter, representing the same width as the ROI, we determined that value as the cutoff value for each patient. As a result, cutoff SUV ranged from 1.93 to 4.47 (mean, 2.31 ± 0.42) in all patients. ROIs for HUA and LUA were placed in tumor regions as close to the brain surface as possible, to allow easy and safe needle biopsy during surgery. The SUV for each ROI was determined automatically. Although we measured both mean and maximal SUVs in the ROI, the present study defined the mean value of the SUV as "SUV". Finally, the ratio of the SUV for the

tumor to the SUV for normal tissue ($SUV_{T/N}$) was calculated for each HUA and LUA.

Sampling of tumor specimens during surgery

For each patient immediately before surgery in the operation room, we stereotactically identified the spatial locations for HUAs and LUAs on a superimposed image combined with a three-dimensional FRP170 PET image with Gd-T1WI, using a surgical navigation system (Stealth Station TRIA plus; Medtronics, Minneapolis, MN), and obtained tumor tissues from each region using previously reported methods [4]. In all cases, the tumor was successfully removed after completing the procedures for specimen sampling.

Immunohistochemical staining of HIF-1α and Ki-67

Tumor specimens obtained from intratumoral regions corresponding to an HUA and LUA on FRP170 PET images for all patients were fixed with 10 % formalin overnight and then embedded in paraffin. For both areas, paraffin-embedded tissue sections (3-µm thick) were collected on 3-aminopropyltriethoxylane-coated glass slides.

The extents of hypoxia and proliferation were estimated from immunohistochemical staining for HIF-1α and Ki-67, respectively. Dewaxed sections were pretreated in a microwave for 30 min in sodium citrate. These preparations were incubated in primary mouse anti-HIF-1α monoclonal antibody (clone, H1alpha67, 1:200; Novus Biologicals, Littleton, CO) and mouse anti-Ki-67 monoclonal antibody (clone, MIB-1, 1:100; Dako Japan, Tokyo, Japan) for 60 min. After incubation in primary antibodies, sections were incubated in peroxidase-conjugated reagents from EnVision kits (Dako Japan) as the secondary antibody, then immersed in diaminobenzidine/H_2O_2 solution for colored visualization of the reaction product. Finally, preparations were counterstained with hematoxylin. Positive staining indices for HIF-1α and Ki-67 were defined as the mean percentage of nuclear-stained cells in approximately 2,000 cells under light microscopy.

Statistical analyses

Mean values for $SUV_{T/N}$ and staining indices for HIF-1α and Ki-67 were compared between HUAs and LUAs using the Mann–Whitney U test. Correlations between staining indices of HIF-1α and Ki-67 were estimated for each HUA and LUA using Pearson's correlation coefficient test. Correlations between $SUV_{T/N}$ values of FRP170 at HUAs and Ki-67 indices in HUAs were assessed in all patients using Pearson's correlation coefficient test. A significant difference was defined as a p value <0.05 in all analyses.

Results

Findings of FRP170 PET

In all patients, HUAs with high accumulation of FRP170 were partially seen in the intermediate layer between the deep layer surrounding the central necrotic region and the outer layer within the peripheral region of the tumor that was involved in region enhancement on Gd-T1WI (Fig. 1b). Fusion images combining Gd-T1WI with FRP170 PET provided localization of both HUA and LUA regions during surgery, and allowed successful sampling of tissues (Fig. 1c, d). No patient developed any complications due to FRP170 PET or tumor tissue sampling. Means (±standard deviation) $SUV_{T/N}$ for HUAs and LUAs were 1.93 ± 0.47 and 1.24 ± 0.14, respectively. A significant difference in mean $SUV_{T/N}$ ($p < 0.001$) was found between HUAs and LUAs (not shown in figures).

HIF-1α and Ki-67

Mean HIF-1α indices were 48.2 ± 9.4 % in HUAs and 19.5 ± 7.5 % in LUAs. Mean HIF-1α index was significantly higher in HUAs than in LUAs ($p < 0.01$, Fig. 2a). Mean Ki-67 indices were 29.8 ± 10.8 % in HUAs and
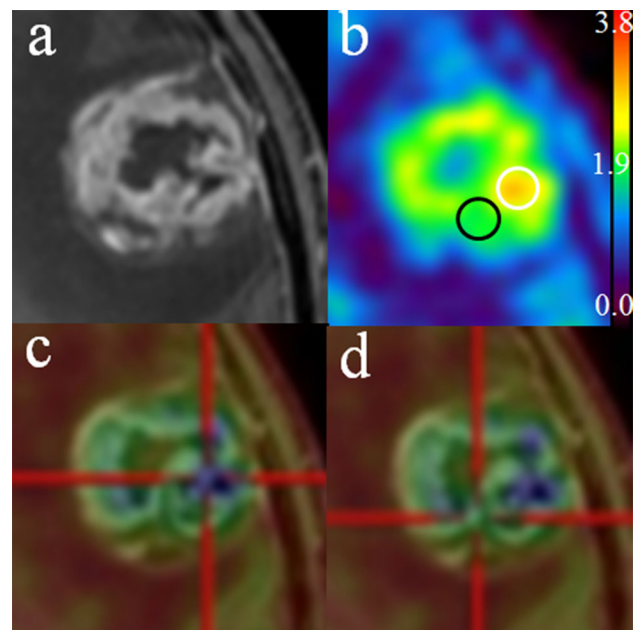

Fig. 1 Gd-T1WI (**a**), FRP170 PET (**b**), and superimposed images combining Gd-T1WI and FRP170 PET (**c**, **d**), showing glioblastoma localized in the left frontal lobe in Case 13. On PET imaging (**b**), ROIs are selected in the HUA (*white circle*) and LUA (*black circle*). On superimposed images, HUA and LUA are depicted as *blue* and *green regions*, respectively. Locations of HUA and LUA were identified stereotaxically. Points of intersection of the *reddish bars* indicate targeted regions of HUA (**c**) and LUA (**d**)

Fig. 2 Comparisons of HIF-1α index (**a**), and Ki67 index (**b**) between HUAs and LUAs
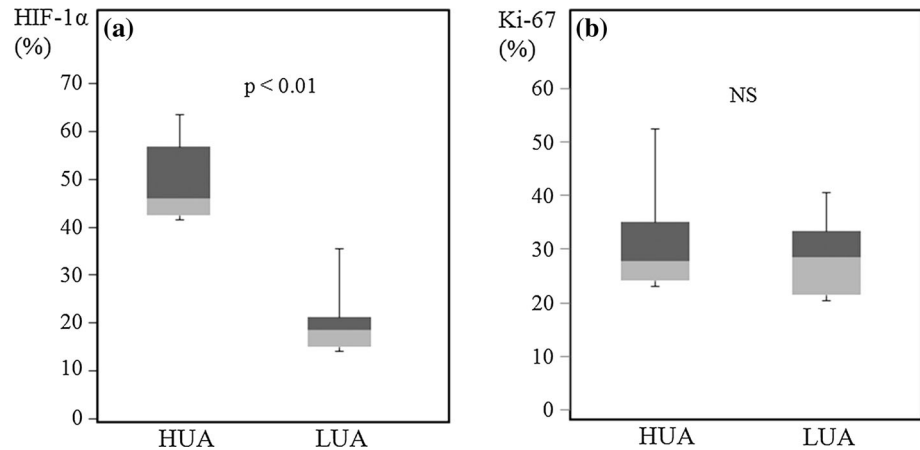
25.8 ± 10.8 % in LUAs. No significant difference in mean Ki-67 index was evident between HUA and LUA ($p = 0.48$, Fig. 2b). No correlations between positive indices of HIF-1α and Ki-67 were found in HUAs ($r = 0.10$, $p = 0.73$) or LUAs ($r = 0.20$, $p = 0.49$). No correlation between $SUV_{T/N}$ values of FRP170 and Ki-67 indices at HUAs was found for any patients.

Discussion

In the present study, significantly higher means of both $SUV_{T/N}$ of FRP170 and nuclear-stained-HIF-1α index in HUAs than in LUAs suggested that the HUA on FRP170 PET represents regions of hypoxic cells within glioblastoma. Both selective accumulation of 2-nitroimidazole derivatives (including FRP170) and nuclear expression of the HIF-1α protein represent active metabolism in barely surviving cells under hypoxic conditions. The former results from chemical metabolism such as a change in the nitroimidazole moiety to radical anions and covalent binding to intracellular macromolecules under hypoxic conditions [6, 8, 20, 21], while the latter is induced by cytological kinetics; HIF-1α protein is phosphorylated and translocated from the cytoplasm to the nucleus only under hypoxic conditions, where it binds to hypoxia-response elements upstream of HIF-1-regulated target genes [22, 23].

The present study showed no significant differences in mean Ki-67 index between HUAs and LUAs. This suggests that HUAs on FRP170 PET certainly include tumor regions retaining proliferative activity. As with our results, no significant differences in Ki-67 positivity were found between HUAs and LUAs on FMISO PET in a glioma rat model [17] and non-small cell lung cancer [18]. However, hypoxia would generally be expected to correlate inversely with proliferation, because the underlying primary cause of cell hypoxia within a tumor is considered to be a wrecked

form after excessive oxygen consumption due to cell proliferation. Locoregional observations using immunohistochemistry have in some reports demonstrated an inverse distribution between hypoxic cells and proliferating cells [14, 19]. Thus, interpreting relationships between hypoxia and proliferation in malignant tumors appears quite complicated [15]. In term of relationships on PET between tracers for hypoxia and proliferation in glioma, only two previous reports have been described, one in vitro [15] and one in vivo [10]. These investigations indicated quantitatively strong correlations in regional uptake values and visually identical distribution between HUAs of hypoxic cell tracers and proliferative activity within gliomas. Causes for the discrepancy that there can be both a co-existence and an inverse distribution between hypoxia and proliferation within a tumor have been reported as differences in experimental models [15, 16], biological heterogeneity within a tumor [24], and hypoxia gradients depending on the distance from necrosis and/or blood vessels [25, 26]. These investigations suggest that proliferating potential is largely affected by hypoxic gradient within the tumor region being observed.

Although reasons why HUAs representing hypoxic areas included regions retaining proliferation in this study have remained unclear, one possible reason is that proliferative potential is likely to be retained in hypoxic cells if cells were not under severe hypoxia. Some previous reports have documented that the co-existence of hypoxic cells and proliferating cells might represent a subpopulation of proliferating cells only under 'intermediate' hypoxic conditions, although relationships between hypoxic and proliferating cells showed an almost inverse correlation in various cancers including brain tumor [27, 28]. Ranges of oxygen pressure (mmHg) in moderate/severe hypoxia, mild hypoxia in glioblastoma, and healthy brain tissue, have been recognized as 0.75–4, 4–20, and 20–100 mmHg, respectively [29]. Accumulation of FMISO is reported to

be increased when hypoxia of <10 mmHg is present in tissue [30]. HUAs on PET with 2-nitroimidazole derivative including FMISO and FRP170 might not only comprise moderately/severely hypoxic cells, but also mildly hypoxic cells in glioblastoma. The wide range of detectable levels of hypoxia on 2-nitroimidazole derivative might be one reason for proliferation within tumor tissue in HUAs representing hypoxia. Another possible reason is that hypoxia itself induces proliferation through activation of hypoxia-responsive elements such as HIF-1α which regulates some aspects such as proliferation, metabolism, and neovascularization [31]. The present study, however, showed no correlation between HIF-1α- and Ki-67-positive indices, suggesting no simultaneous interaction between these two factors. Another possible reason is the influence of hypoxia on the cell cycle. Hypoxia induces cell cycle arrest or delays the cell cycle for tumor cell viability, increasing cell populations in the G_0/G_1 and G_2/M phase [32, 33]. Accumulation of cells in states of arrested or delayed cycling could lead to a false proliferation rate and, consequently, might have shown co-existence of hypoxia and proliferation in histological observations.

Some limitations regarding the study results must be considered. First, the sample size of this study was small. Additional studies with a larger number of patients with glioblastoma are needed. Second, the SUV cutoff to determine the HUA on each PET was not fixed a standard value for all patients, because no cutoff value has been established for clear differentiation between HUA and LUA. Third, maximum SUVs in this study were not evaluated using an ROI smaller than 10 mm in diameter. We thought a simple protocol would be optimal in this study, combining mean SUV with histological features from a large ROI, as the risk of tissue sampling error would be greater in a small ROI than in a large ROI. Fourth, although this study suggested the co-existences of HIF-1α- and Ki-67-stained cells in HUAs, the co-expression or co-accumulation of both parameters in individual cells was not extensively evaluated. Further investigations examining the co-existence of two parameters for hypoxia and proliferation in individual cells may, therefore, explain the results obtained.

Conclusion

We observed immunochemical staining for HIF-1α and Ki-67 in surgical specimens sampled from each HUA and LUA on FRP170 PET in patients with glioblastoma. Mean HIF-1α-positive indices were significantly higher in HUA than in LUA, whereas no significant difference was observed in mean Ki-67-positive indices between HUA and LUA. That is, HUAs on FRP170 PET clearly represent hypoxic areas in glioblastoma, but HUAs does not necessarily suggest low proliferation potential even though proliferation is generally considered to be inversely correlated with hypoxia. Although we speculated about the reasons for this apparent contradiction, further research in this area needs to be accumulated.

References

1. Jensen RL. Hypoxia in the tumorigenesis of gliomas and as a potential target for therapeutic measures. Neurosurg Focus. 2006;20(4):E24.
2. Rich JN. Cancer stem cells in radiation resistance. Cancer Res. 2007;67(19):8980–4.
3. Mendichovszky I, Jackson A. Imaging hypoxia in gliomas. Br J Radiol. 2011;84:S145–58 Spec No 2.
4. Beppu T, Terasaki K, Sasaki T, Fujiwara S, Matsuura H, Ogasawara K, et al. Standardized uptake value in high uptake area on positron emission tomography with 18F-FRP170 as a hypoxic cell tracer correlates with intratumoral oxygen pressure in glioblastoma. Mol Imag Biol. 2014;16:127–35.
5. Ishikawa Y, Iwata R, Furumoto S, Takai Y. Automated preparation of hypoxic cell marker [18F]FRP-170 by on-column hydrolysis. Appl Radiat Isot. 2005;62(5):705–10.
6. Kaneta T, Takai Y, Iwata R, Hakamatsuka T, Yasuda H, Nakayama K, et al. Initial evaluation of dynamic human imaging using 18F-FRP170 as a new PET tracer for imaging hypoxia. Ann Nucl Med. 2007;21(2):101–7.
7. Kaneta T, Takai Y, Kagaya Y, Yamane Y, Wada H, Yuki M, et al. Imaging of ischemic but viable myocardium using a new 18F-labeled 2-nitroimidazole analog, 18F-FRP170. J Nucl Med. 2002;43(1):109–16.
8. Shibahara I, Kumabe T, Kanamori M, Saito R, Sonoda Y, Watanabe M, et al. Imaging of hypoxic lesions in patients with gliomas by using positron emission tomography with 1-(2-[18F]fluoro-1-[hydroxymethyl]ethoxy)methyl-2-nitroimidazole, a new 18F-labeled 2-nitroimidazole analog. J Neurosurg. 2010;113(2):358–68.
9. Eschmann SM, Paulsen F, Reimold M, Dittmann H, Welz S, Reischl G, et al. Prognostic impact of hypoxia imaging with 18F-misonidazole PET in non-small cell lung cancer and head and neck cancer before radiotherapy. J Nucl Med. 2005;46(2):253–60.
10. Kawai N, Maeda Y, Kudomi N, Miyake K, Okada M, Yamamoto Y, et al. Correlation of biological aggressiveness assessed by 11C-methionine PET and hypoxic burden assessed by 18F-fluoromisonidazole PET in newly diagnosed glioblastoma. Eur J Nucl Med Mol Imaging. 2011;38(3):441–50.
11. Swanson KR, Chakraborty G, Wang CH, Rockne R, Harpold HL, Muzi M, et al. Complementary but distinct roles for MRI and 18F-fluoromisonidazole PET in the assessment of human glioblastomas. J Nucl Med. 2009;50(1):36–44.

12. Narita T, Aoyama H, Hirata K, Onodera S, Shiga T, Kobayashi H, et al. Reoxygenation of glioblastoma multiforme treated with fractionated radiotherapy concomitant with temozolomide: changes defined by 18F-fluoromisonidazole positron emission tomography: two case reports. Jpn J Clin Oncol. 2012;42(2):120–3.

13. Heijmen L, Ter Voert EG, Punt CJ, Heerschap A, Oyen WJ, Bussink J, et al. Monitoring hypoxia and vasculature during bevacizumab treatment in a murine colorectal cancer model. Contrast Media Mol Imaging. 2014;9(3):237–45.

14. Tanaka T, Furukawa T, Fujieda S, Kasamatsu S, Yonekura Y, Fujibayashi Y. Double-tracer autoradiography with Cu-ATSM/FDG and immunohistochemical interpretation in four different mouse implanted tumor models. Nucl Med Biol. 2006;33(6): 743–50.

15. Dence CS, Ponde DE, Welch MJ, Lewis JS. Autoradiographic and small-animal PET comparisons between (18)F-FMISO, (18)F-FDG, (18)F-FLT and the hypoxic selective (64)Cu-ATSM in a rodent model of cancer. Nucl Med Biol. 2008;35(6):713–20.

16. Rajendran JG, Mankoff DA, O'Sullivan F, Peterson LM, Schwartz DL, Conrad EU, et al. Hypoxia and glucose metabolism in malignant tumors: evaluation by [18F]fluoromisonidazole and [18F]fluorodeoxyglucose positron emission tomography imaging. Clin Cancer Res. 2004;10(7):2245–52.

17. Hatano T, Zhao S, Zhao Y, Nishijima K, Kuno N, Hanzawa H, et al. Biological characteristics of intratumoral [F-18]fluoromisonidazole distribution in a rodent model of glioma. Int J Oncol. 2013;42(3):823–30.

18. Cherk MH, Foo SS, Poon AM, Knight SR, Murone C, Papenfuss AT, et al. Lack of correlation of hypoxic cell fraction and angiogenesis with glucose metabolic rate in non-small cell lung cancer assessed by 18F-Fluoromisonidazole and 18F-FDG PET. J Nucl Med. 2006;47(12):1921–6.

19. Evans SM, Jenkins KW, Chen HI, Jenkins WT, Judy KD, Hwang WT, et al. The relationship among hypoxia, proliferation, and outcome in patients with de novo glioblastoma: a pilot study. Transl Oncol. 2010;3(3):160–9.

20. Chapman JD. Hypoxic sensitizers–implications for radiation therapy. New Engl J Med. 1979;301(26):1429–32.

21. Krohn KA, Link JM, Mason RP. Molecular imaging of hypoxia. J Nucl Med. 2008;49(Suppl 2):129S–48S.

22. Wang GL, Semenza GL. Purification and characterization of hypoxia-inducible factor 1. J Biol Chem. 1995;270(3):1230–7.

23. Fischer I, Gagner JP, Law M, Newcomb EW, Zagzag D. Angiogenesis in gliomas: biology and molecular pathophysiology. Brain Pathol. 2005;15(4):297–310.

24. Denekamp J, Dasu A. Inducible repair and the two forms of tumour hypoxia–time for a paradigm shift. Acta Oncol. 1999;38(7):903–18.

25. Raleigh JA, Zeman EM, Calkins DP, McEntee MC, Thrall DE. Distribution of hypoxia and proliferation associated markers in spontaneous canine tumors. Acta Oncol. 1995;34(3):345–9.

26. Ljungkvist AS, Bussink J, Rijken PF, Kaanders JH, van der Kogel AJ, Denekamp J. Vascular architecture, hypoxia, and proliferation in first-generation xenografts of human head-and-neck squamous cell carcinomas. Int J Radiat Oncol Biol Phys. 2002;54(1):215–28.

27. Evans SM, Hahn SM, Magarelli DP, Koch CJ. Hypoxic heterogeneity in human tumors: eF5 binding, vasculature, necrosis, and proliferation. Am J Clin Oncol. 2001;24(5):467–72.

28. Hoogsteen IJ, Marres HA, Wijffels KI, Rijken PF, Peters JP, van den Hoogen FJ, et al. Colocalization of carbonic anhydrase 9 expression and cell proliferation in human head and neck squamous cell carcinoma. Clin Cancer Res. 2005;11(1):97–106.

29. Evans SM, Jenkins KW, Jenkins WT, Dilling T, Judy KD, Schrlau A, et al. Imaging and analytical methods as applied to the evaluation of vasculature and hypoxia in human brain tumors. Radiat Res. 2008;170(6):677–90.

30. Rasey JS, Hofstrand PD, Chin LK, Tewson TJ. Characterization of [18F]fluoroetanidazole, a new radiopharmaceutical for detecting tumor hypoxia. J Nucl Med. 1999;40(6):1072–9.

31. Rankin EB, Giaccia AJ. The role of hypoxia-inducible factors in tumorigenesis. Cell Death Differ. 2008;15(4):678–85.

32. Schmaltz C, Hardenbergh PH, Wells A, Fisher DE. Regulation of proliferation-survival decisions during tumor cell hypoxia. Mol Cell Biol. 1998;18(5):2845–54.

33. Webster L, Hodgkiss RJ, Wilson GD. Cell cycle distribution of hypoxia and progression of hypoxic tumour cells in vivo. Br J Cancer. 1998;77(2):227–34.